IR spectroscopy and OH⁻ in silicate garnet: The long quest to document the hydrogarnet substitution⚑

Charles A. Geiger[1,*] and George R. Rossman[2]

[1]Department of Chemistry and Physics of Materials, Division Materials Science and Mineralogy, Salzburg University, Jakob Haringer Strasse 2a, A-5020 Salzburg, Austria

[2]Division of Geological and Planetary Sciences, California Institute of Technology, Pasadena, California 91125-2500, U.S.A.

Abstract

There has been much research undertaken on structural OH⁻ in various nominally anhydrous minerals including the common silicate garnets (i.e., $X_3Y_2Si_3O_{12}$, where $X = Mg$, Fe^{2+}, Mn^{2+}, and Ca and $Y = Al$, Fe^{3+}, and Cr^{3+}). However, it is still largely not understood where small concentrations of H atoms are incorporated in the garnet crystal structure. In this work, the IR single-crystal spectra of end-member or approaching end-member composition andradite, pyrope, and almandine are measured. Both a natural and synthetic andradite sample show a broad, asymmetric OH⁻-stretching mode at 3563 cm⁻¹ that splits into two narrower modes at lower temperatures. They are located at 3575 and 3557 cm⁻¹ at 80 K with the higher wavenumber mode being considerably more intense compared to that at lower energy. These results are analyzed together with published IR spectra of synthetic end-member katoite, pyrope, and almandine also recorded at low temperature. These garnets show similar IR behavior with a broad OH⁻ band at room temperature that splits into two narrower bands at lower temperatures and with a similar intensity relationship as shown by andradite. This behavior is indicative of the hydrogarnet substitution. The measured IR spectra of natural almandine- and pyrope-rich (Dora Maira, Italy) crystals, on the other hand, show different spectroscopic features with several OH⁻ modes that are not consistent with the hydrogarnet mechanism. An analysis of the energy of the OH⁻-stretching mode is made for various composition hydrogarnet clusters [i.e., $X_3Y_2(O_4H_4)_3$, where $X = Mg$, Fe^{2+}, Mn^{2+} and Ca and $Y = Al$ and Fe^{3+}] in terms of crystal-chemical properties and local atomic configurations. The OH⁻ mode energy, which lies roughly between 3660 and 3550 cm⁻¹ at RT for various end-member garnets, is a function of the mass of the X- and Y-cations due to mode coupling and/or mixing. In addition, the strength of the chemical bonding between the X- and Y-cations and the O^{2-} anion of the OH⁻ dipole plays a role in affecting the wavenumber of the OH⁻-stretching vibration. OH⁻ mode broadening, observed in the spectra of end-member garnets, is primarily a result of thermal anharmonic disorder, especially with regard to the light H cation. OH mode broadening in intermediate solid-solution composition garnets is a function of both thermal effects and variations in local cation configurations around the OH⁻ dipole(s). Published IR spectra of certain high-pressure pyrope-rich garnets, both synthetic and natural, are analyzed and arguments made that OH⁻ can often be incorporated as the hydrogarnet or hydropyrope substitution. IR spectra similar in appearance, having multiple relatively narrow OH⁻ modes that are distinct from those indicating the hydrogarnet substitution, can be observed for certain synthetic end-member and various composition natural pyropes from Dora Maira and some natural spessartines. This indicates that other common OH⁻ substitution mechanisms, which have yet to be determined, can also occur in different silicate garnets.

Keywords: Hydrogarnet, silicate garnet, OH⁻ in minerals, IR spectroscopy, crystal chemistry; Water in Nominally Hydrous and Anhydrous Minerals

Introduction

There has been much research undertaken on structural OH⁻ in nominally anhydrous minerals. Several different rock-forming silicates, for instance, have been shown to contain OH⁻ in various, yet minor concentrations. There can be important geological consequences (Keppler and Smyth 2006). For example, there has been discussion on how many "oceans of water" could be present in Earth's mantle (Bell and Rossman 1992a) with its implications for global geochemical and geophysical processes. One notable class of silicates that has received much study is the common silicate garnets ($X_3Al_2Si_3O_{12}$ where $X = Mg$, Fe^{2+}, Mn^{2+}, Ca; $Y = Al$, Fe^{3+}, Cr^{3+}), and they have been shown to have different OH⁻ concentrations arising from various unknown substitution mechanisms. At low concentration, some researchers speak of OH⁻ defects.

* E-mail: ca.geiger@sbg.ac.at

It terms of studying structural OH⁻, IR single-crystal spectroscopy is generally the analytical method of choice, because the OH⁻ dipole is strongly IR active. The IR spectra of a large number of natural garnets have been recorded (e.g., Aines and Rossman 1984; Rossman and Aines 1991; Bell and Rossman 1992; Matsyuk et al. 1998). In spite of this, surprisingly, at least to the non-expert, is the fact that it is not understood where or how small concentrations of H^+ atoms are incorporated structurally in the various garnet species. This determination is not easily made, because the OH⁻-stretching modes cannot be straightforwardly assigned. In addition, some garnets, such as grossular-katoite compositions especially, show a great variability in the number of their OH⁻ modes (Rossman and Aines 1991). Of course, diffraction experiments could theoretically give H positions in a crystal (e.g., Cohen-Addad et al. 1967; Lager et al. 1987), but at low-concentration levels this is not possible. Proton NMR study of synthetic hydrogrossular and three natural grossulars showed in some cases the presence of four H-atom clusters (hydrogarnet) and also two H-atom clusters (Cho and Rossman 1993). Computations have not advanced to the stage that IR or NMR spectra can be calculated well enough to interpret the experimental results precisely. In terms of interpreting IR spectra and assigning OH⁻ modes, presently one is stuck with empirical-based comparisons of spectra from different garnets and the possible conclusions that derive from them.

The simple, standard starting point for interpreting IR spectra begins with the classic hydrogarnet substitution (Aines and Rossman 1984). That is, one substitutes locally an $O_4H_4^{4-}$ "group" (see Kolesov and Geiger 2005, for a discussion of OH⁻ mode behavior in katoite) for a SiO_4^{4-} one in the silicate garnet crystal structure. The idea derives from early work showing the existence of "hydrogarnet." Indeed, end-member katoite, $Ca_3Al_2O_{12}H_{12}$, can be synthesized in the laboratory and it shows complete solid solution with grossular (Flint et al. 1941). This substitution mechanism is, because so little is understood, the starting point or "fallback position" that is often used when attempting to interpret the IR spectra of some silicates and especially silicate garnet (Aines and Rossman 1984) with low OH⁻ contents. It remains, however, just an unproven assumption. It can be concluded, at the present time, that it is not understood precisely how minor OH⁻ is structurally contained in garnet both synthetic and natural.

A major obstacle in understanding the nature of OH⁻ in garnet is that natural crystals are normally solid-solution compositions and, moreover, they have also experienced relatively complex geologic P-T histories. Thus, investigations have been made on synthetic crystals that have simpler chemistries and that can be grown under well controlled P_{H_2O}-T conditions (e.g., Geiger et al. 1991, 2000, 2018; Armbruster and Geiger 1993; Withers et al. 1998; Mookherjee and Karato 2010). Indeed, the results show that synthetic garnets often, but not always, show simpler IR spectra compared to those of naturals. Another approach is to measure the spectra of nearly end-member natural garnets with the hope that they will be simpler than crystals with more complex compositions. These two considerations are one of the modus operandi for the present work.

We present and analyze the IR single-crystal spectra of natural nearly end-member andradite, pyrope, and almandine garnets. The spectra are then compared with their equivalent synthetic crystals that were grown at high pressure and high temperature in the laboratory. OH⁻ mode behavior for the hydrogarnet substitution in the various end-member garnets is interpreted for the first time by considering crystal-chemical properties and the local atomic configurations around an OH⁻ dipole. This type of analysis is used further in an attempt to assign different OH⁻ modes in spectra of various intermediate composition high-pressure synthetic and natural pyrope-rich garnets.

SAMPLES AND EXPERIMENTAL METHODS

Garnet samples

The various garnet crystals, both synthetic and natural, measured via IR spectroscopy in this study are described in Table 1. The precise outcrop locations for three of the pyrope crystals are given in Simon and Chopin (2001) and their compositions in Geiger and Rossman (1994). The natural near end-member andradite is from Val Malenco, Italy (collection of GRR) and the synthetic andradite crystal is described in Armbruster and Geiger (1993) and Geiger et al. (in press). In terms of almandine, three different natural samples, belonging to the some of the most almandine-rich crystals found to date, were studied. The geologic occurrence and mineralogical characterization of two of them are discussed in Woodland et al. (1995) and Aparicio et al. (2012). For IR investigation, the

TABLE 1. Description of natural and synthetic garnet samples measured in this study

Sample label	Locality (source)/synthesis conditions	Sample description and composition	Mol% (±1–2) End-member composition
Pyrope MAS-2a	Masueria, Italy (Ch. Chopin; Simon and Chopin 2001; Geiger and Rossman 1994)	Pinkish to light red transparent single crystal containing various inclusions.	Py(76)
Pyrope MAS-2b	Masueria, Italy (Ch. Chopin; Simon and Chopin 2001; Geiger and Rossman 1994)	Very light pinkish transparent single crystal.	Py(99)
Pyrope SB	San Bernardo, Italy (Ch. Chopin; Simon and Chopin 2001; Geiger and Rossman 1994)	Light pinkish transparent single crystal.	Py(82)
Pyrope Ch-2	"Dora Maira", Italy (Ch. Chopin, exact locality unknown; Geiger and Rossman 1994)	Colorless transparent single crystal.	Py(98)
Andradite #27	T = 1200 °C, P = 20 kbar, w/PtO₂ (Armbruster and Geiger 1993; Geiger et al. 2018)	Loose synthetic polycrystalline product (An₁₀₀) with some individual crystals up to roughly 300 μm in size. Yellow greenish to golden in color. Isotropic.	An(100)
Andradite GRR-134	Val Malenco, Italy (Amthauer and Rossman 1998)	Light green transparent single crystal. Anisotropic.	An(99)
Almandine A-5	Collobrières, France (C. Ferraris, Paris, Muséum national d'histoire naturelle, Geiger and Rossman 1994)	Single crystals millimeter size. Compositionally homogeneous and unzoned. Inclusions.	Al(94)
Almandine FR-3	Collobrières, France (Woodland et al. 1995)	Crystals up to centimeter size. Metamorphosed ironstone. Compositionally homogeneous and unzoned. Numerous cracks and some inclusions.	Al(93)
Almandine JF-1	Zlaty Chlum near Jesenik, Czech Republic (Aparicio et al. 2012)	Metasedimentary rocks (Soucek 1978).	Al(95)

crystals were slightly ground to two parallel sides to produce thin crystal platelets and then finely polished.

FTIR single-crystal spectroscopy

For the IR single-crystal measurements, the preparation and experimental conditions are similar to those described in Aines and Rossman (1984) and Geiger et al. (1991). A few spectra were obtained with a Thermo-Nicolet iS50 FTIR with a Continuμm microscope accessory with a cryogenic MCT-A detector and a CaF$_2$ beam splitter. Most spectra were collected, though, by attaching the doubly polished crystal platelets over metal pinhole apertures of appropriate size (200–600 μm) and measuring directly in the IR spectrometer sample compartment with an InSb detector. The sample holder was carefully aligned to yield the strongest signal. Multiple spectra were collected on different crystal regions that were clear and transparent under the binocular microscope and free from any observable inclusions.

Low-temperature spectra were collected using a Continuμm infrared microscope with a 15× objective and a cryogenic HgCdTe detector. Samples were cooled with liquid nitrogen in a Linkam FTIR 600 stage.

RESULTS

Andradite

The IR spectra of natural end-member andradite (GRR-134) from Val Malenco, Italy, from 296 K down to 80 K are shown in Figure 1. The broad asymmetric OH$^-$ band with a peak maximum at 3563 cm^{-1} at room temperature (RT) splits into two OH$^-$ bands that narrow and the more intense band increases slightly in wavenumber with decreasing temperature. At 80 K, the two peak maxima are located at 3575 and 3557 cm^{-1}. Very weak bands appear at higher wavenumbers in the spectrum at 80 K. The RT spectrum of synthetic andradite (And 27) is the same as the natural crystal in terms of the OH$^-$ band placement (Fig. 1).

Pyrope

The IR spectra of four different composition pyrope-rich solid-solution crystals from different geographic locations in the general area of Dora Maira, Italy, are shown in Figure 2. They are shown with generally decreasing pyrope contents from bottom to top. There is a broadening of the OH$^-$ bands as one moves away from close to end-member pyrope into more intermediate compositions. The spectrum of sample Masueria 2b with the most intense OH$^-$ modes shows five well-resolved OH$^-$ bands located at 3660, 3651, 3641, 3618 (weak), and 3602 cm^{-1} and a slight shoulder on the high wavenumber side of the mode at 3660 cm^{-1}. The other pyropes show broadly similar spectra.

Almandine

The spectra for the three different almandine samples (Table 1) are shown in Figure 3. The IR spectrum of the almandine (FR-3) from Collobrières, France, as described by Woodland et al. (1995), is characterized by an OH$^-$ band doublet showing possible minor structure. The two main peaks have maxima at 3641 and 3623 cm^{-1}. There is also the possible presence of very weak OH$^-$ bands (doublet) centered around ~3590 cm^{-1}. The spectrum of almandine from Zlaty Chlum near Jesenik, Czech Republic (JF-1), shows weak OH$^-$ bands at 3562, 3523, 3501, and 3454 cm^{-1}. Another almandine crystal from Collobrières, France (A-5), shows very weak OH bands similar in energy to those of the Zlaty Chlum sample.

DISCUSSION

IR spectra of compositionally end-member or nearly end-member garnets

Synthetic and natural andradite. The IR spectrum of end-member andradite (synthetic and natural) shows a broad asymmetric mode OH$^-$ at 3563 cm^{-1} that splits into two narrower modes at lower temperatures. We note that other natural andradite crystals can show spectra with more than one OH$^-$ band
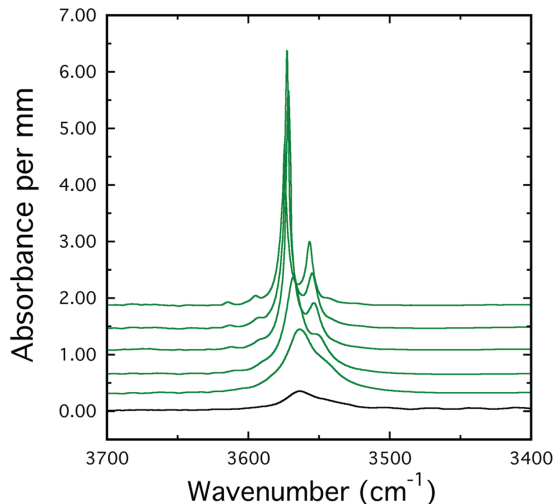

FIGURE 1. IR single-crystal spectra of natural end-member andradite from Val Malenco, Italy (Table 1), at 296, 198, 123, 89, and 80 K (from bottom to top). The broad asymmetric OH band at room temperature has a peak maximum at 3563 cm^{-1} and two major peaks at 3575 and 3557 cm^{-1} at 80 K. The RT spectrum of synthetic andradite no. 27 (black) is shown at the bottom (Geiger et al. 2018) also with a single band at 3563 cm^{-1} at RT.
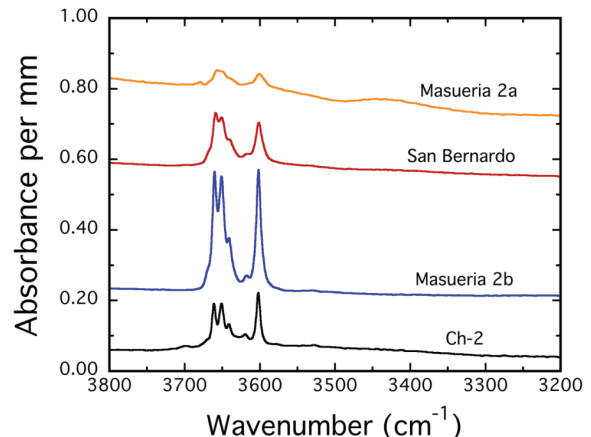

FIGURE 2. IR single-crystal spectra of various composition pyrope-rich crystals from Dora Maira, Italy (Table 1). They are shown with increasing almandine and slight grossular contents (decreasing pyrope component) from bottom to top. For the most "water-rich" crystal (Masueria 2b) the five main OH band energies are at 3660, 3651, 3641, 3618 (weak), and 3602 cm^{-1} and a weak shoulder on the high-energy wing of the band at 3660 cm^{-1}. The OH modes broaden with decreasing pyrope content in more intermediate compositions due to variations in local atomic configurations (see text).
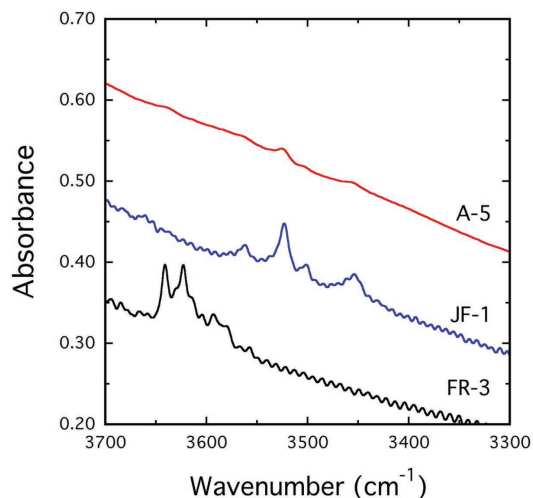
FIGURE 3. IR single-crystal spectra of the three almandine-rich crystals (Table 1). Sample FR-3 is 0.30 mm, sample A-5 0.22 mm, and sample JF-1 0.36 mm thick. The sloping background is due to the low-energy flank of an intense electronic transition related to Fe^{2+} that is centered at about 4400 cm^{-1} (Geiger and Rossman 1994). The OH⁻ band energies are given in the text.

(Amthauer and Rossman 1998; Adamo et al. 2011; Geiger et al. 2018), but many show this intense band at 3563 cm^{-1}.

Natural pyrope. Garnet crystals from the Dora Maira, Italy, area are unique in terms of composition (Chopin 1984; Simon and Chopin 2001), some being very close to end-member pyrope; $Mg_3Al_2Si_3O_{12}$ (e.g., Masueria 2b/MAS2b and Ch-2; Table 1). There is, though, a range of compositional variability involving solid solution with almandine and grossular ($[Mg,Fe^{2+},Ca]_3Al_2Si_3O_{12}$) giving, for example, crystals with about 76 mol% pyrope (i.e., sample Masueria 2a/MAS 2a; Table 1). Pyrope-rich garnets from Earth's mantle have entirely different petrologic origins and ranges of composition, containing considerably more grossular and almandine, as well as sometimes knorringite, components (e.g., Bell and Rossman 1992; Matsyuk et al. 1998, as discussed below). The spectra of the four different crystals from Dora Maira are similar to those presented in Rossman et al. (1989), who listed four OH⁻ bands at 3661.5, 3651.0, 3641.3, and 3602.1 cm^{-1}. The measurements herein confirm this, but we find, in addition, a weak OH⁻ mode at 3618 cm^{-1} as well as a slight shoulder on the high wavenumber side of the mode at 3660 cm^{-1}. There is a clear broadening of the OH⁻ bands with increasing almandine and grossular content in the garnet (Fig. 2; spectra bottom to top). The OH⁻ peak intensities are different among the four samples indicating variable OH⁻ concentrations.

Natural almandine. Three different natural almandine samples were examined and they represent some of the most $Fe_3Al_2Si_3O_{12}$-rich crystals that have been studied to date (cf. sample JF-1, Table 1, was first studied by IR spectroscopy by Aparicio et al. 2012). The crystals of JF-1 and A-5 show similar IR spectra with OH modes at about 3562, 3523, 3501, and 3454 cm^{-1} (Fig. 3). The spectrum of almandine FR-3 is different and is characterized by two narrow higher energy bands at 3641 and 3623 cm^{-1}. All three garnets show very different OH⁻ modes than the less almandine-rich Wrangell sample in Aines and Rossman

(1984), whose IR spectrum was proposed to represent "typical" almandine. The intensity of the OH⁻ bands in all these almandines is weak. The presented spectra show the most OH⁻-rich parts of various crystals, as some other recorded spectra show barely visible OH⁻ bands or none at all (i.e., there are variations in the OH⁻ contents). Low OH⁻ contents appear to be a general characteristic of many natural almandine crystals (also unpublished results of C.A.G and G.R.R.).

An analysis of OH⁻-mode behavior in the IR spectra of garnet

The hydrogarnet substitution in end-member garnets. Over the years, the IR spectra of a large number of garnets, both natural and synthetic, have been measured. In many cases, the observed OH⁻ stretching bands, which may be one or more in number and showing a range of wavenumbers, have been suggested to represent the hydrogarnet substitution (e.g., Aines and Rossman 1984; Geiger et al. 1991; Withers et al. 1998). However, the underlying scientific arguments for these proposals are effectively nonexistent for anything other than hydrogrossular (katoite), itself. We think, though, that progress in this question can be made using the IR results from this work, together with spectra of other garnets given in the literature, by analyzing the nature of the OH⁻ bands in terms of the structural and crystal-chemical properties of garnet.

To start the analysis, we consider the IR spectrum of synthetic katoite, $Ca_3Al_2O_{12}H_{12}$, a non-silicate garnet, which has been studied at temperatures from 293 K (RT) down to 10 K (Kolesov and Geiger 2005). Its OH⁻-mode behavior is well documented and understood at least between 293 and 80 K. The spectrum of katoite shows a single intense and broad asymmetric OH⁻-stretching mode at 3662 cm^{-1} at RT, which narrows and shifts to higher energies with decreasing temperature. With further decreasing temperature and first at about 80 K, a second much less intense OH⁻-stretching mode at about 3600 cm^{-1} appears. This two OH⁻-band pattern characterizes the IR spectrum of katoite with the notable addition of weaker fine structure appearing on these two strongest modes below about 80 K. The nature of these fine structure OH⁻ modes is not understood.

The IR spectrum of both natural end-member (Val Malenco) and synthetic andradite are the same in terms of the energy of the single asymmetric OH⁻ mode occurring at 3563 cm^{-1}. This agreement is notable and has not been observed before for other natural and synthetic end-member garnet species to the best of our knowledge. With decreasing temperature, this OH⁻ band begins to narrow and it splits into a more intense higher energy mode and a less intense mode at low wavenumbers (Figs. 1 and 4). We think this behavior reflects the hydrogarnet substitution in andradite for two reasons. First, it is similar to that observed for katoite upon cooling. Second, both natural end-member and synthetic andradite show the same IR spectrum. Thus, it can largely be ruled out that OH⁻ defects, related to the presence of other garnet chemical components, especially those containing highly charged elements (e.g., Ti^{4+}; see below), are not found in significant amounts in both garnets. *P* and *T* conditions of formation between the two samples are also widely different. The synthetic was grown at 1200 °C (Geiger and Armbruster 1997), whereas the natural crystal comes from a much lower temperature serpentinite.

This interpretation for the IR hydrogarnet signature is further supported by the spectra of most synthetic hydrothermally grown pyropes recorded at RT and 80 K (Geiger et al. 1991, see, however, discussion below on other synthetic pyrope crystals). Once again, a relatively broad asymmetric OH⁻ mode at 3629 cm⁻¹, at RT splits upon cooling into two narrow bands at 80 K (3638 and 3614 cm⁻¹; Fig. 4) and they show a similar intensity relationship as the OH⁻-mode doublet in katoite and andradite. Synthetic almandine shows a more complex IR spectrum with two broad OH⁻ bands at RT (Fig. 4), but the most intense OH⁻ band at 3613 cm⁻¹, which we assign to the hydrogarnet substitution, behaves in a similar manner (Geiger et al., in preparation) as the three garnets discussed above. At 80 K, three narrow OH⁻ bands derive from the RT band at 3613 cm⁻¹. However, the typical "hydrogarnet" doublet occurs once again and is the most prominent of the three bands. Finally, the assignment of the respective OH⁻ modes to a hydrogarnet substitution in the various end-member garnet species is consistent with their wavenumber behavior as based on their structural and crystal-chemical properties, as discussed next.

The cubic silicate garnet structure, space group $Ia\bar{3}d$, is characterized by three cation sites (X, Y, and Si) located on special crystallographic sites and a single oxygen anion located at a general position (i.e., it has positional freedom in x, y, and z). Katoite has the same space group and, here, the Si cation is absent and is charged balanced by the presence locally of four H⁺ cations (i.e., the so-called hydrogarnet substitution). Figure 5 shows the local atomic environment around a single OH⁻ group that serves as one dipole of the hydrogarnet O_4H_4 cluster without a neighboring Si cation. The oxygen anion is bonded to one Y cation, two X cations, and the H atom. The bond with H gives the stretching vibration of the OH⁻ dipole that is so strongly IR active. It has been argued or implied in various works that the energy of this OH stretching mode depends on the OH···O length in the garnet, that is, the strength of the hydrogen bonding. The relationship between OH···O bond length and the vibrational stretching energy of the OH⁻ bond for many different compounds is well known (e.g., Nakamoto et al. 1955; Libowitzky 1999). The analyses show that the OH⁻ stretching energy is not a meaningful function of the H···O length, when it is greater than about 2.0 Å. In other words, OH⁻ vibrational energies between roughly 3500 and 3700 cm⁻¹ do not give any unique information on the H···O bond length. Indeed, a free OH⁻ dipole is considered to vibrate at approximately 3560 cm⁻¹ (Libowitzky 1999). Thus, it makes no sense to argue that the varying OH⁻-mode wavenumbers observed for the different end-member garnets are related to differences in H-bonding lengths (i.e., H bonding is stronger in OH⁻-bearing andradite than in OH⁻-bearing pyrope, for example). The lack of measurable hydrogen bonding in garnet is shown, moreover, by the IR spectra made as a function of temperature. For katoite, andradite, pyrope, and almandine, the most intense OH⁻ mode increases in energy with decreasing temperature, whereas the general observation for H-bonded systems should be just the opposite, namely H-bonding increases in strength with decreasing temperature.

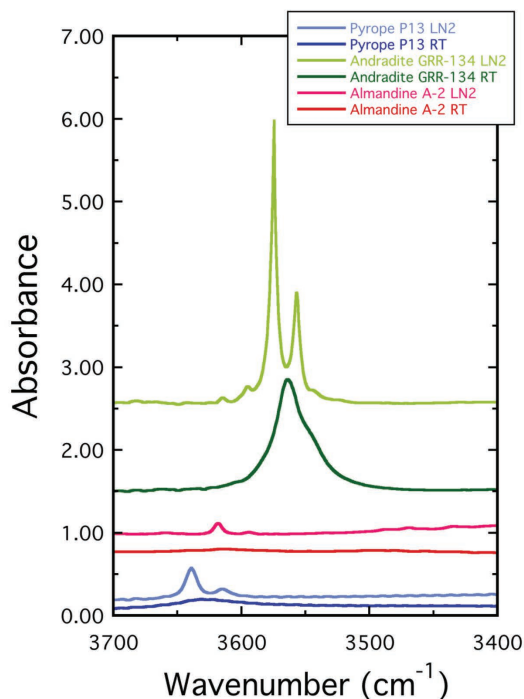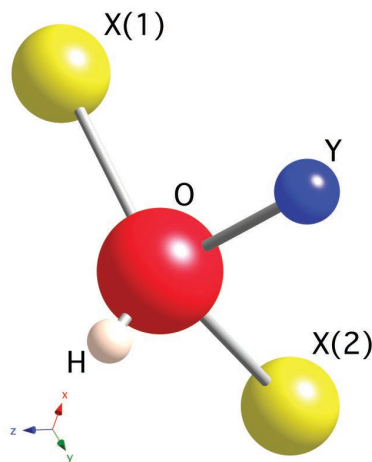We think, instead, that the OH⁻-bearing vibrational energy

FIGURE 4. Comparison of IR spectra of end-member synthetic pyrope (sample P-13, 0.273 mm thick, from Geiger et al. 1991), almandine (A-2, ~0.90 mm thick, in Geiger et al., in preparation) and natural andradite (GRR-134, 1.185 mm thick, this work) at room temperature and ~80 K (liquid N₂). For synthetic pyrope the OH band at 3629 cm⁻¹ at RT splits into two narrow OH bands at 3638 and 3614 cm⁻¹. For synthetic almandine the most intense broad OH band at 3613 cm⁻¹ at RT splits into three narrow OH bands at 3663 (weakest), 3617 (intense), and 3590 (weak) cm⁻¹ at about 80 K with the latter two assumed to represent the hydrogarnet substitution.

FIGURE 5. Local atomic environment around a single O anion in the case of katoite (no Si cation). The oxygen anion (red) in the garnet structure is bonded to one Y(Al) cation (blue), two X(Ca) cations [yellow; in hydrogrossular with bond lengths of Ca1-O(1) = 2.462(3) Å, Ca(2)-O(4) = 2.520(3) Å (Lager et al. 2002), and a H atom (pink)].

in the different end-member garnets is largely a function of two crystal-chemical properties. The first is atomic mass. Because the O^{2-} anion in hydrogarnet is bonded to three cations and the H atom (Fig. 5), whereby the former cations are considerably heavier, the energy of the OH^- stretching vibration will be affected via mode coupling through the O^{2-} anion. That is, the heavier the combined mass of the X- and Y-cations, the lower the energy of the OH^- mode. The second important crystal-chemical effect involves the strength of the X(1)-O, X(2)-O, and Y-O bonds. The stronger they are, the weaker the OH^- bond will be. This general effect is, for example, well documented in crystal hydrates containing an alkali or alkaline-earth cation that is bonded to the oxygen anion of an H_2O molecule (Lutz 1988). The observation is, the stronger the cation-oxygen interaction, the weaker the intramolecular OH^- bond (i.e., lower energy) of the H_2O molecule. In terms of chemical bonding in silicate garnets it has been shown, using calculated bond valences, that Ca-O bonding in andradite is stronger than Fe^{2+}-O bonding in almandine and Mg-O bonding in pyrope (Armbruster and Geiger 1993). Thus, the OH bond in andradite will be weakened compared to that of the latter two garnets.

Consider the bond effect in garnet further. Rossman and Aines (1991) argued that end-member katoite and OH^--poor grossular components in a $Ca_3Al_2(SiO_4)_{1-x}(O_4H_4)_x$ solid-solution crystal are characterized by two OH^- stretching modes at 3660 and 3598 cm^{-1} at RT, respectively. At first glance, this might appear to be at odds with the analysis given above, because the local atomic configuration for a hydrogrossular and katoite cluster might be considered the same (Fig. 5). However, only the masses of atoms in the clusters are the same but not the Ca-O bond lengths. In silicate grossular the Ca-O bond lengths are Ca(1)-O(4) = 2.322(1) Å and Ca(2)-O(4) = 2.487(1) Å (Geiger and Armbruster 1997) and in end-member katoite Ca(1)-O(4) = 2.465(2) Å and Ca(2)-O(4) = 2.511(1) Å (Lager et al. 1987). Ca-O bonding is stronger in grossular than in katoite (this analysis ignores, of course, the fact that the Ca-O bonds in a local hydrogrossular cluster should be a bit longer than the Ca-O bonds in the much more prevalent silicate grossular "matrix." That is, there is local bond relaxation in the solid solution). Summarizing, OH^- bonding will be weaker for hydrogrossular-like clusters than for katoite clusters in a $Ca_3Al_2(SiO_4)_{1-x}(O_4H_4)_x$ solid-solution crystal.

The above analysis does not consider thermal effects, which are clearly reflected in the temperature-dependent IR measurements. Indeed, diffraction measurements made on katoite (Foreman 1968; Cohen-Addad et al. 1967; Lager et al. 1987, 2002) at RT show that the H/D atoms are characterized by large amplitudes of vibration and we think this dynamic behavior causes the OH^- mode broadening. Atomic amplitudes of vibration, especially for the light H atom, are damped at lower temperatures, resulting in substantial OH^- mode narrowing and then splitting. Kolesov and Geiger (2005) analyzed the nature of OH^- mode widths for both IR and Raman spectra in the case of katoite. It can be argued that the natural (non thermal) half widths for OH modes are less than 20 cm^{-1} at temperatures below 10 K.

In conclusion, an analysis of the wavenumber behavior for the single OH^- stretching mode at RT, arising from the presence of hydrogarnet ($O_4H_4^{4-}$) groups in various garnets, shows

that it should decrease, as observed, in the order katoite (3662 cm^{-1}), pyrope (3629 cm^{-1}), almandine (3613 cm^{-1}), grossular (3598 cm^{-1}), and andradite (3563 cm^{-1}).

OH^--mode widths and energies in end-member and intermediate composition garnets

The half-widths of the OH^- stretching band are greater for intermediate composition natural garnets with two or more different X-cations compared to those of end-member or nearly end-member compositions having just one predominant X-cation (e.g., Aines and Rossman 1984). The modes are broader because of the presence of different local-cation distributions. That is, static related local-atomic and local-structural heterogeneity contributes to mode broadening in addition to atomic thermal effects. This can be illustrated by considering the possible nature of cation mixing at the X-site, as in a hypothetical $[Mg,Fe^{2+},Ca]_3Al_2Si_3O_{12}$ aluminosilicate garnet (Fig. 6). This figure shows an edge-shared dodecahedral (D)-tetrahedral (T) chain (Fig. 6a) with a hypothetical distribution of three different X-cations and a local T-D cluster (Fig. 6b) in the garnet structure, respectively. Every SiO_4 or O_4H_4 group in garnet has two edge-shared and four corner-shared dodecahedra (a single OH^- dipole of an O_4H_4 group is illustrated in Fig. 5). In the case of an end-member garnet, the local X-cation environment around every $O_4H_4^{4-}$ group/OH^- dipole is the same (i.e., there is no local compositional and structural heterogeneity). However, in the case of intermediate composition garnets there should be a range of $O_4H_4^{4-}$ groups or OH^- dipoles associated with different local X-cation configurations. Each local-atomic configuration will be characterized by its own "static" structural properties, for example, bond lengths and angles (see, e.g., Armbruster and Lager 1989) that vary with the sizes of the cations involved (see general discussion in Bosenick et al. 2000, and Freeman et al. 2006).

In addition, the masses of the X-cations in the various configurations will be different. These local variations in structural properties and masses will give rise to a distribution of OH^- stretching band mode energies (the situation is, for example, not totally dissimilar to that in the amphiboles, which are much better understood in terms of their OH^- mode behavior, see e.g., Hawthorne and Della Ventura 2007. Here, separate OH^- modes can even be used to describe the distribution of different cations in neighboring M sites). In other words, in terms of Figure 6a and with a typical pyrope-rich mantle garnet, for example, there will be statistically a large fraction of local D(Mg)-T-D(Mg) configurations, but also D(Mg)-T-D(Fe^{2+}), D(Mg)-T-D(Ca), D(Ca)-T-D(Fe^{2+}), D(Ca)-T-D(Ca), and D(Fe^{2+})-T-D(Fe^{2+}) ones. Their relative percentage will depend on the bulk composition of the crystal and also, importantly, on any energetically preferred configurations (i.e., possible short-range cation ordering; see Palke et al. 2015). The latter effect is complex in nature and not understood for garnet. Indeed, there could well be certain preferred local atomic configurations (O_4H_4 or SiO_4 groups surrounded by a non-random distribution of X-cations) in intermediate composition garnets. Of the various silicate garnet species, it is only grossular (and possibly andradite) that shows complete solid solution with a hydrogarnet end-member (Flint et al. 1941). Pyrope and almandine, in comparison, show much
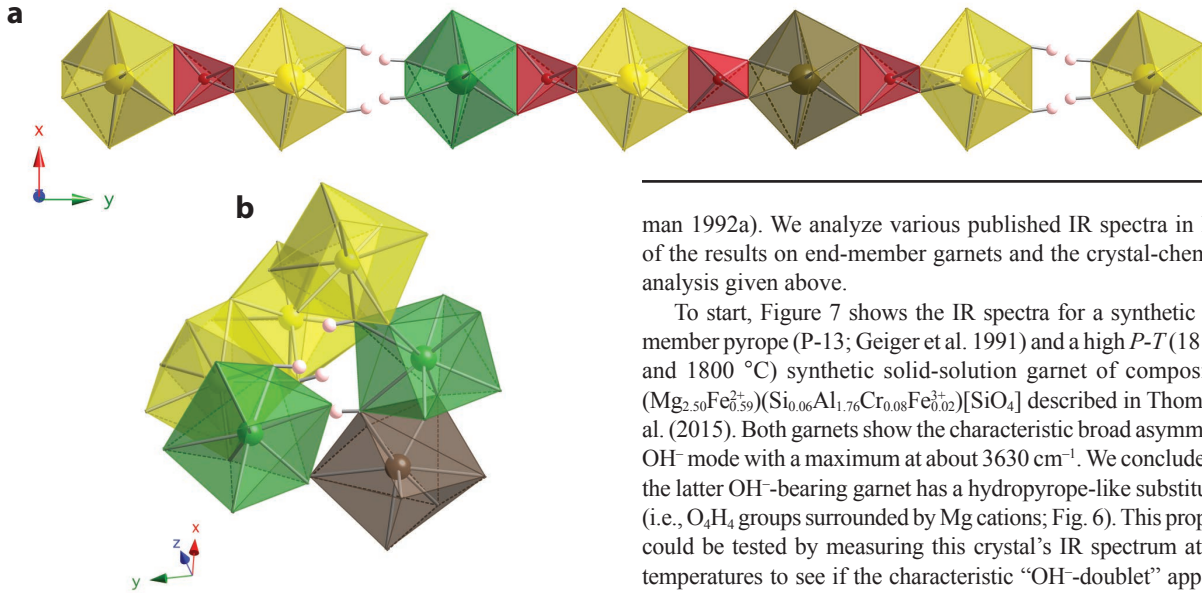
FIGURE 6. (**a**) Hypothetical tetrahedral-dodecahedral "chain" that could be found in a Mg-Fe-Ca intermediate composition garnet. Both O_4H_4 (H atoms are the pinkish-colored spheres) and SiO_4 (red) "tetrahedra" are shown. For example, in the case of a pyrope-rich solid-solution crystal, the yellow spheres would represent Mg, brown Fe^{2+} and green Ca. (**b**) One hypothetical local divalent X-cation environment around an O_4H_4 group in garnet. The oxygen anions from each of the four OH^- dipoles form the central tetrahedron and they can be bonded locally to different combinations of X-cations. This can lead to OH^- mode broadening in solid-solution crystals (see text).

less tendency toward a hydrogarnet solid solution. The simple crystal-chemical interpretation for this is that garnets with the larger Ca cation, and a concomitant larger unit-cell volume (e.g., grossular; 12.529 J/bar vs. pyrope; 11.316 J/bar and almandine; 11.523 J/bar), offer a more "expanded crystal structure" that allows for considerable incorporation of the larger O_4H_4 groups.

In conclusion, this crystal-chemical-based analysis offers a framework to begin to interpret OH^- mode energies and widths related to various hydrogarnet components in both end-member and intermediate composition garnets. Former works that simply considered a specific OH^- mode energy or energies among different garnet species and their compositions to identify, say a common hydrogarnet substitution, are based on wrong premises. Such a simple analysis cannot be correct. A first attempt to assign OH^- IR modes for the hydrogarnet substitution in intermediate garnets, as well as understanding the physical nature of their energies, will now be made.

The hydrogarnet and other OH^- substitutional mechanisms in high-pressure garnets

Considerable effort has focused on investigating OH^- in synthetic (Geiger et al. 1991; Withers et al. 1998; Mookerjee and Karato 2010; Thomas et al. 2015) and natural (Bell and Rossman 1992b; Matsyuk et al. 1998) high-pressure garnets, because the question of the bulk water content in Earth's interior is of great geochemical and geophysical interest (Bell and Ross-

man 1992a). We analyze various published IR spectra in light of the results on end-member garnets and the crystal-chemical analysis given above.

To start, Figure 7 shows the IR spectra for a synthetic end-member pyrope (P-13; Geiger et al. 1991) and a high P-T (18 GPa and 1800 °C) synthetic solid-solution garnet of composition $(Mg_{2.50}Fe^{2+}_{0.59})(Si_{0.06}Al_{1.76}Cr_{0.08}Fe^{3+}_{0.02})[SiO_4]$ described in Thomas et al. (2015). Both garnets show the characteristic broad asymmetric OH^- mode with a maximum at about 3630 cm^{-1}. We conclude that the latter OH^--bearing garnet has a hydropyrope-like substitution (i.e., O_4H_4 groups surrounded by Mg cations; Fig. 6). This proposal could be tested by measuring this crystal's IR spectrum at low temperatures to see if the characteristic "OH^--doublet" appears. The IR spectra of other majorite-containing garnets in Thomas et al. (2015) show different spectra that, in some cases, may reflect variations in composition and, thus, local cation configurations.

The IR spectra of natural pyrope garnets are different in appearance. Many various composition pyrope-rich garnets, deriving from different mantle-rock types, were studied spectroscopically in detail by Bell and Rossman (1992b) and Matsyuk et al. (1998). There is, in general, good agreement in the observations from both investigations, which are more mineralogical-petrological in nature and where assignments of the OH^- modes were not made. OH^--mode behavior is analyzed, here, using structural and crystal-chemical properties as introduced above.
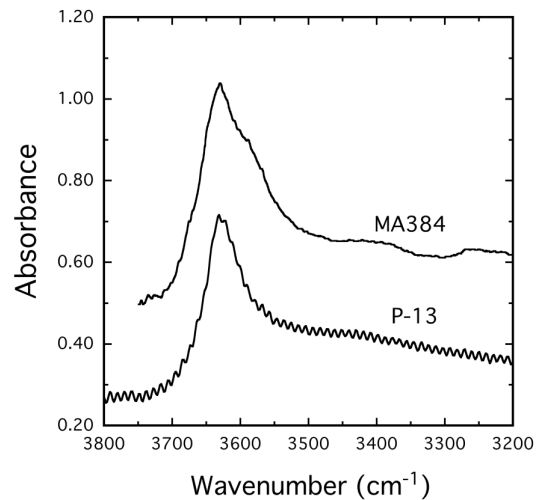

FIGURE 7. IR spectra of $Mg_3Al_2Si_3O_{12}$ (P-13; Geiger et al. 1991) synthesized at P_{H_2O} = 2.3 Ga and T = 1100 °C and garnet of composition $(Mg_{2.50}Fe^{2+}_{0.59})(Si_{0.06}Al_{1.76}Cr_{0.08}Fe^{3+}_{0.02})Si_3O_{12}$ (spectrum MA384 digitized from Thomas et al. 2015, with absorbance divided by 30) synthesized at P_{H_2O} = 18 GPa and T = 1800 °C (with 0.5 L H_2O added). The OH^- band defines a local hydropyrope cluster in both crystals.

Presently, it is not understood why natural pyropes show spectra with two or three or more OH⁻ modes and with wavenumbers different than that of the single OH⁻ mode at 3629 cm⁻¹ observed for most synthetic pyropes. Bell and Rossman divide their studied garnets, based on their characteristic IR spectra and OH⁻ mode energies and intensities, into three groups, namely "high-, middle-, and low-wavenumber" types. Matsyuk et al. propose a similar classification with three main spectral groups labeled as I, II, and III, as characterized by their OH⁻-mode wavenumbers of 3645–3662, 3561–3583, and 3515–3527 cm⁻¹, respectively.

The IR spectra of three different pyropes from mantle xenoliths (LAC-40, Lace, S. Africa; RTF-2 and RTF-4, Rietfontein; Bell and Rossman 1992b) are shown in Figure 8. We start our analysis with garnet RTF-2 that shows an asymmetric OH⁻ mode with a maximum at about 3650 cm⁻¹. It could potentially, based on the arguments made above, represent a hydrogarnet substitution. However, its wavenumber is greater than any OH⁻ mode measured in any end-member silicate garnet. Therefore, at first glance, it could be concluded that it does not represent a hydrogarnet substitution. However, there is explanation for its high wavenumber and it follows from an analysis of X-O bond lengths in binary $X_3Al_2Si_3O_{12}$ garnet solid solutions (Bosenick et al. 2000; Freeman et al. 2006; Geiger 2008). We propose that this OH⁻ mode at roughly 3650 cm⁻¹ represents a hydropyrope-like
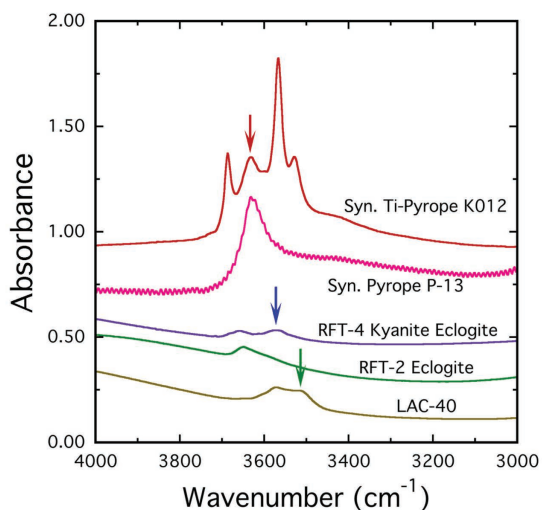

FIGURE 8. Comparison of IR spectra of two synthetic and three natural pyropes. The synthetic Ti-bearing pyrope is from Geiger et al. (2000) and end-member pyrope from Geiger et al. (1991). The IR spectra for the three natural pyropes are from Bell and Rossman (1992b, note that the IR spectra for RTF-2 and RTF-4 are interchanged in their work). The garnets show their three different wavenumber types "high, middle, and low" or the I, II, and III groups of Matsyuk et al. (1998). The three types or groups are marked by red, blue, and green arrows, respectively. The red arrow marks a possible local hydropyrope cluster in the garnet (about 3630 cm⁻¹ in the synthetics and 3650 cm⁻¹ in the natural solid solution RTF-2). The blue arrow marks a possible hydrogrossular-like cluster in RTF-4 and LAC-40 (at about 3570 cm⁻¹). The green arrow marks an OH⁻ mode possibly related to the presence of Ti in garnet. See text for further discussion.

cluster in a solid-solution silicate garnet crystal. The OH⁻ mode is greater by about 20 cm⁻¹ wavenumbers than that for the OH⁻ mode in end-member pyrope (3629 cm⁻¹), because the associated Mg-O bonds in the hydropyrope cluster will be slightly greater in length compared to those in end-member silicate pyrope (note also that the wavenumber difference between the OH⁻ mode for katoite and OH⁻-poor grossular (locally hydrogrossular clusters) is about 60 cm⁻¹). That is, the presence of significant amounts of Ca in the garnet solid solution act to expand the average unit-cell volume compared to that in end-member pyrope and the Mg-O bonds will be slightly lengthened accordingly. It follows, then, that the OH⁻ stretching mode in a local hydropyrope cluster in a solid-solution crystal will be stronger and, thus, will vibrate at a higher energy compared to the case of a local hydropyrope cluster in nearly end-member pyrope.

Most mantle pyrope-rich garnets, though, are marked by the most intense OH⁻ mode located at approximately 3570 cm⁻¹ (middle-wavenumber type of Bell and Rossman or group II of Matsyuk et al. 1998; Fig. 8 samples RTF-4 and LAC 40; and also see spectra "a" and "p" in Fig. 2 of Bell and Rossman 1992). We assign this mode to a hydrogrossular-like-cluster contained in a pyrope-rich solid-solution crystal. The Ca-O bonds in the hydrogrossular cluster will be slightly shorter compared to those clusters in nearly end-member grossular and, thus, stronger. Therefore, the OH⁻ bond will be weaker and its stretching energy will lie at lower wavenumbers compared to OH⁻ in nearly end-member grossular (i.e., 3598 cm⁻¹). The mass effect seems to play a secondary role in affecting the energy of this OH⁻ mode in the pyrope-rich solid solutions. Bell and Rossman (1992; p. 169) write "Preliminary indications are that the position of this band maximum shifts in a regular fashion to lower wavenumber as a function of decreasing Mg/(Mg+Fe) ratio in megacrysts." We interpret this as indicating that the local hydrogrossular-like-clusters are becoming statistically slightly more Fe^{2+} rich (Fig. 6b). Finally, it is important to note that this band at 3570 cm⁻¹ is often the most intense OH⁻ mode observed in the spectra of mantle pyropes (Bell and Rossman 1992). We think this is reflecting the fact that a hydrogrossular cluster is energetically more favorable than, say, a hydropyrope cluster in a solid-solution garnet for the crystal-chemical reasons discussed above.

To end the analysis, we address the third major OH⁻ mode type that can observed in mantle pyropes. It is located at roughly 3512 cm⁻¹ (Bell and Rossman 1992) or between 3515–3527 cm⁻¹ (Matsyuk et al. 1998). The latter workers argue that his mode is associated with relatively TiO_2-rich garnets (about >0.4 wt%). This proposal is consistent with the IR spectra of synthetic Ti-bearing pyropes that have multi-OH-band spectra and show a low-energy mode at 3526 cm⁻¹ (Fig. 8 of Geiger et al. 2000). It is also notable that these synthetic Ti-bearing pyropes show a broad OH⁻ mode at about 3630 cm⁻¹ at RT (Fig. 8), which splits into two narrow bands at 78 K (Geiger et al. 2000).

Other non-hydrogarnet OH⁻ substitutional mechanisms in end-member garnet

The results and analysis given above are a strong argument that the hydrogarnet substitution can occur in several end-member or nearly end-member silicate garnets and that it is characterized by a single, broad OH⁻ mode at RT. However,

some nearly end-member natural garnets can also show more complex multi-OH⁻-band spectra, where the bands are relatively narrow and have energies unlike those garnets containing a hydrogarnet component (almandine, this work; pyrope, this work and Rossman et al. 1989; grossular, Rossman and Aines 1991; spessartine, Aines and Rossman 1984). The immediate conclusion is that there must be other structural or defect mechanisms for incorporating OH⁻ in garnet. Figure 9 shows the IR spectrum of a nearly end-member pyrope (i.e., Masueria 2b, see Table 1), a synthetic pyrope grown from a gel-starting material (Geiger et al. 1991), and a natural nearly end-member spessartine (Rutherford Mine, Amelia Courthouse, Amelia Co., Virginia). All three garnets show similar IR patterns with the same number of five OH⁻ bands and having a similar wavenumber distribution (The OH⁻ modes in spessartine lie at lower energies because, again, Mn^{2+} is heavier than Mg^{2+}.) The only difference is in the relative intensities among some of the bands. These three garnets apparently have OH⁻ located at common structural sites and they are different than that of the "standard" hydrogarnet substitution. The narrow half widths of the OH⁻ bands further characterize the spectra of these garnets and it can be argued that the vibrational freedom of the OH groups is more restricted compared to that for OH⁻ groups in the hydrogarnet substitution.

IMPLICATIONS

A long and continuing goal in the investigation of H_2O at low concentrations in nominally anhydrous silicates is to assign different vibrational OH⁻ stretching modes to various substitutional mechanisms and structural sites. The spectroscopic and crystal-chemical analysis undertaken in this work is a step in this direction. The results show that for silicates with relatively complex structu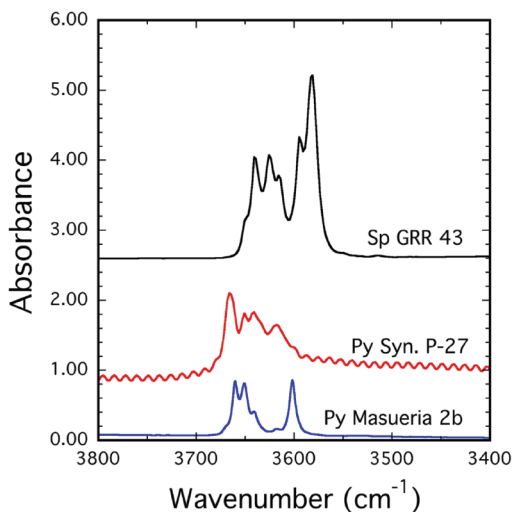res more effort must be made to understand local crystal-chemical properties and atomic configurations in the immediate vicinity of any OH⁻ groups. This is necessary to interpret both the possible number of OH⁻ modes as well as their energies. It follows, conversely, that it may be possible in some cases to use OH⁻-stretching modes in nominally anhydrous minerals as a probe to investigate the nature of short-range-atomic order in intermediate solid-solution compositions (cf. to the case of OH⁻-bearing minerals; Hawthorne and Della Ventura 2007).

The role of atoms occurring in minor concentrations in garnet, especially those that lead to deviations in the nonstoichiometry of the formula unit from 3:2:3:12 (e.g., Na, B, Li, Zr, P, F), as well as possible point defects, and their possible effect on OH⁻ incorporation, needs further study. Work on compositionally simpler, well-characterized synthetic crystals will be essential in this regard. Also important to consider is the role of trivalent cation substitutions at the tetrahedral site, where H^+ may act as the charge-compensation ion associated with a single OH⁻ group.

Finally, the results and proposals, herein, could be of significance in terms of efforts to quantify the small concentrations of OH⁻ in garnet solid solutions. It can be expected that molar absorption coefficients for OH⁻ could be a function of the local structural type of OH⁻. Existing calibrations with a single absorption coefficient, based on several OH⁻ modes deriving from different OH⁻ sites or groups (e.g., hydropyrope, hydrogrossular, hydrospessartine), may not be quantitative. It could be expected that each OH⁻ substitution mechanism (i.e., with different dipole interactions) will have its own characteristic molar absorption coefficient. This appears to be the case with olivine (Kovács et al. 2010). Concentrating calibration work just on the mode (or modes) related to a hydrogarnet substitution (or different local hydrogarnet substitutions in solid-solution crystals), as outlined herein, could permit a better understanding of OH⁻ concentration as a function of P-T-X crystallization conditions. Of course, any analytical method giving bulk OH⁻ contents could be difficult to interpret.

REFERENCES CITED

Adamo, I., Bocchio, R., Diella, V., Pavese, A., Vignola, P., Prosperi, L., and Palamza, V. (2009) Dematoid from Val Malenco, Italy: Review and update. Gems and Gemology, 45, 280–287.
Adamo, I., Gatta, G.D., Rotiroti, N., Diella, V., and Pavese, A. (2011) Green andradite stones: gemmological and mineralogical characterisation. European Journal of Mineralogy, 23, 91–100.
Aines, R.D., and Rossman, G.R. (1984) The hydrous component in garnets: pyralspites. American Mineralogist, 69, 1116–1126.
Amthauer, G., and Rossman, G.R. (1998) The hydrous component in andradite garnet. American Mineralogist, 83, 835–840.
Aparicio, C., Filip, J., Skogby, H., Marusak, Z., Mashlan, M., and Zboril, R. (2012) Thermal behavior of almandine at temperatures of 1,200°C in hydrogen. Physics and Chemistry of Minerals, 39, 311–318.
Armbruster, T., and Geiger, C.A. (1993) Andradite crystal chemistry, dynamic X-site disorder and strain in silicate garnets. European Journal of Mineralogy, 5, 59–71.
Armbruster, T., and Lager, G.A. (1989) Oxygen disorder and the hydrogen position in garnet-hydrogarnet solid solution. European Journal of Mineralogy, 1, 363–369.
Bell, D.R., and Rossman, G.R. (1992a) Water in Earth's mantle: the role of nomi-

FIGURE 9. IR spectra of natural end-member spessartine (GRR-43; 0.271 mm), natural end-member pyrope (Masueria 2b; 2.308 mm) and pyrope synthesized from a gel (Py-27 in Geiger et al. 1991, normalized to 5.0 mm). The latter has bands at 3663, 3651, 3641, and 3618 and a low-energy shoulder at 3604 cm⁻¹ and also a weak shoulder on the high-energy wing of the band at 3663 cm⁻¹.

nally anhydrous minerals. Science, 255, 1391–1397.

——— (1992b) The distribution of hydroxyl in garnets from the subcontinental mantle of southern Africa. Contributions to Mineralogy and Petrology, 111, 161–178.

Bosenick, A., Dove, M.T., and Geiger, C.A. (2000) Simulation studies of pyrope-grossular solid solutions. Physics and Chemistry of Minerals, 27, 398–418.

Cho, H., and Rossman, G.R. (1993) Single-crystal NMR studies of low-concentration hydrous species in minerals: Grossular garnet. American Mineralogist, 78, 1149–1164.

Chopin, C. (1984) Coesite and pure pyrope in high-grade blueschists of the Western Alps: a first record and some consequences. Contributions to Mineralogy and Petrology, 86, 107–118.

Cohen-Addad, C., Ducros, P., and Bertaut, E.F. (1967) Étude de la substitution du groupement SiO_4 par $(OH)_4$ dans les composés $Al_2Ca_3(OH)_{12}$ et $Al_2Ca_3(SiO_4)_{2.16}(OH)_{3.36}$ de type grenat. Acta Crystallographica, 23, 220–230.

Flint, E.P., McMurdie, H.F., and Wells, L.S. (1941) Hydrothermal and X-ray studies of the garnet-hydrogarnet series and the relationship of the series to hydration products of portland cement. Journal of Research of the National Bureau of Standards, 27, 171–180.

Foreman, D.W. Jr. (1968) Neutron and X-ray diffraction study of $Ca_3Al_2(O_4D_4)_3$, a garnetoid. The Journal of Chemical Physics, 48, 3037–3041.

Freeman, C.L., Allan, N.L., and van Westrenen, W. (2006) Local cation environments in the pyrope-grossular $Mg_3Al_2Si_3O_{12}$-$Ca_3Al_2Si_3O_{12}$ garnet solid solution. Physical Review, 74, 134203.

Geiger, C.A. (2008) Silicate garnet: A micro to macroscopic (re)view. American Mineralogist, 93, 360–372.

Geiger, C.A., and Armbruster, T. (1997) $Mn_3Al_2Si_3O_{12}$ spessartine and $Ca_3Al_2Si_3O_{12}$ grossular garnet: dynamical structural and thermodynamic properties. American Mineralogist, 82, 740–747.

Geiger, C.A., and Rossman, G.R. (1994) Crystal field stabilization energies of almandine-pyrope and almandine-spessartine garnets determined by FTIR near infrared measurements. Physics and Chemistry of Minerals, 21, 516–525.

Geiger, C.A., Langer, K., Bell, D.R., Rossman, G.R., and Winkler, B. (1991) The hydroxide component in synthetic pyrope. American Mineralogist, 76, 49–59.

Geiger, C.A., Stahl, A., and Rossman, G.R. (2000) Single-crystal IR- and UV/VIS-spectroscopic measurements on transition-metal-bearing pyrope: The incorporation of hydroxide in garnet. European Journal of Mineralogy, 12, 259–271.

Geiger, C.A., Dachs, E., Vielreicher, N.M., and Rossman, G.R. (2018) Heat capacity behavior of andradite: A multi-sample and -methodological investigation. European Journal of Mineralogy, in press.

Hawthorne, F.C., and Della Ventura, G. (2007) Short-range order in amphiboles. In F.C. Hawthorne, R. Oberti, G. Della Ventura, and A. Mottana, Eds., Amphiboles: Crystal Chemistry, Occurrence, and Health Issues, 67, p. 173–222. Reviews in Mineralogy and Geochemistry, Mineralogical Society of America, Chantilly, Virginia.

Keppler, H., and Smyth, J.R. (2006) Water in nominally anhydrous minerals. Reviews in Mineralogy and Geochemistry, 62, 169–191.

Kolesov, B.A., and Geiger, C.A. (2005) The vibrational spectrum of synthetic hydrogrossular (katoite) $Ca_3Al_2(O_4H_4)_3$: A low temperature IR and Raman spectroscopic study. American Mineralogist, 90, 1335–1341.

Kovács, I., O'Neill, H.St.C., Hermann, J., and Hauri, E. (2010) Site-specific infrared O-H absorption coefficients for water substitution into olivine. American Mineralogist, 95, 292–299.

Lager, G.A., Armbruster, T., and Faber, G. (1987) Neutron and X-ray diffraction study of hydrogarnet $Ca_3Al_2(O_4H_4)_3$. American Mineralogist, 72, 756–765.

Lager, G.A., Downs, R.T., Origlieri, M., and Garoutte, R. (2002) High-pressure single-crystal X-ray study of katoite hydrogarnet: Evidence for a phase transition from $Ia3d \rightarrow I\bar{4}3d$ symmetry at 5 GPa. American Mineralogist, 87, 642–647.

Libowitzky, E. (1999) Correlation of O-H stretching frequencies and O-H…O hydrogen bond lengths in minerals. Monatshefte für Chemie, 130, 1047–1059.

Lutz, H.D. (1988) Bonding and structure of water molecules in solid hydrates. Correlation of spectroscopic and structural data. Structure and Bonding, 69, 97–125.

Matsyuk, S.S., Langer, K., and Hösch, A. (1998) Hydroxyl defects in garnets from mantle xenoliths in kimberlites of the Siberian platform. Contributions to Mineralogy and Petrology, 132, 163–179.

Mookherjee, M., and Karato, S. (2010) Solubility of water in pyrope-rich garnet at high pressures and temperature. Geophysical Research Letters, 37, 1–5.

Nakamoto, K., Margoshes, M., and Rundle, R.E. (1955) Stretching frequencies as a function of distances in hydrogen bonds. Journal of American Chemical Society, 77, 6480–6486.

Palke, A.C., Stebbins, J.F., Geiger, C.A., and Tippelt, G. (2015) Cation order-disorder in Fe-bearing pyrope and grossular garnets: An ^{27}Al and ^{29}Si MAS NMR and ^{57}Fe Mössbauer spectroscopy study. American Mineralogist, 100, 536–547.

Rossman, G.R., and Aines, R.D. (1991) The hydrous components in garnets: Grossular-hydrogrossular. American Mineralogist, 76, 1153–1164.

Rossman, G.R., Beran, A., and Langer, K. (1989) The hydrous component of pyrope from the Dora Maira Massif, Western Alps. European Journal of Mineralogy, 1, 151–154.

Simon, G., and Chopin, C. (2001) Enstatite-sapphirine crack-related assemblages in ultrahigh-pressure pyrope megablasts, Dora Maira Massif, western Alps. Contributions to Mineralogy and Petrology, 140, 422–440.

Soucek, J. (1978) Metamorphic zones of the Vrbno and Rejviz Series, the Hruby Jesenik Mountains, Czechoslovalia. Tschermaks Mineralogische und Petrographische Mitteilungen, 25, 195–217.

Thomas, S-M., Wilson, K., Koch-Müller, M., Hauri, E.H., McCammon, C., Jacobsen, S.D., Lazarz, J., Rhede, D., Ren, M., Blair, N., and Lenz, S. (2015) Quantification of water in majoritic garnet. American Mineralogist, 100, 1084–1092.

Withers, A.C., Wood, B.J., and Carroll, M.R. (1998) The OH content of pyrope at high pressure. Chemical Geology, 147, 161–171.

Woodland, A.B., Droop, G., and O'Neill, H.St.C. (1995) Almandine-rich garnet from Collobrières, southern France, and its petrological significance. European Journal of Mineralogy, 7, 187–194.